NEW DEVICES AND METHODS OF MEASUREMENT

Linear induction accelerators—new generators of high power relativistic electron beams

Yu. P. Vakhrushin and I. M. Matora
D. V. Efremov Scientific Research Institute of Electro-Physical Apparatus, Leningrad; Joint Institute for Nuclear Research, Dubna
Usp. Fiz. Nauk **110**, 117-137 (May 1973)

Use of the first operating linear induction accelerators (LIA) in the USA and the USSR has shown that the principle on which the operation of these accelerators is based permits relativistic electron beams of hundreds or thousands of amperes to be obtained with efficiencies of tens of percent with high reliability and reproducibility of the results. A number of laboratories are carrying on intensive development of accelerators of this type and developing their theory, methods of calculation, and refinement of the designs. The present review systematizes and generalizes the results of published articles in this field. The article discusses the theory of LIA, the shape of the accelerating field, and the containment of the transverse dimensions of a high-current beam. The parameters are given for accelerators in operation and under construction and the design of the basic elements is described.

CONTENTS

1. INTRODUCTION

The development of research in the field of controlled thermonuclear fusion[1] and new methods of acceleration[2] has led to the building in the sixties of new linear accelerators of high-power relativistic electron beams[3-5], whose principle of operation was proposed by Bowersy[6] at the end of the nineteen thirties.

Use of these so-called linear induction accelerators (LIA) has already permitted studies to be carried on in the Astron program[7] in the USA and the well known Dubna experiments on collective acceleration in the USSR[8-11].

Operation of the first two working LIA (Figs. 1 and 2) has shown that this very simple method of acceleration is promising since it permits obtaining relativistic beams of hundreds or thousands of amperes with efficiencies of tens of percent with high reliability and reproducibility. A number of laboratories are already carrying out intensive development of LIA[12-18], their theory, method of calculation, and refinement of the designs. Studies are being made of iron-free and plasma accelerators of this type[19-23].

This review systematizes and generalizes the results of papers known to the authors in this new field of accelerator technology.

2. PRINCIPLE OF OPERATION

Figure 3 shows the construction of an LIA induction system and makes clear the principle of operation of the accelerator. On variation of the magnetic flux in the cores, a rotational electric field ($\nabla \times \mathbf{E} \neq 0$) is excited in the accelerator tube in accordance with the law of

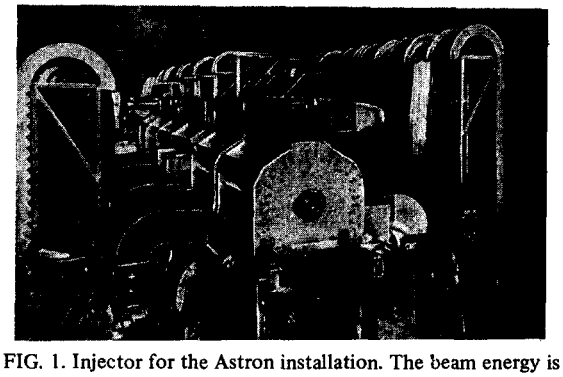

FIG. 1. Injector for the Astron installation. The beam energy is 3.7 MeV, and the current 350 A.

magnetic induction. If the system is sufficiently long, the average electric field strength E_0 on the axis can be written in the form

$$E_0 = -(N/\mathscr{L})\, S\, \partial B/\partial t, \qquad (1)$$

or

$$E_0 = NU_1/\mathscr{L}, \qquad (2)$$

where N is the number of cores, S is the cross section of one core, B is the magnetic field strength in the cores, averaged over the cross section, U_1 is the voltage applied to the primary winding, $\mathscr{L}$ is the length of the system, and $\partial B/\partial t$ is the rate of change of the magnetic field strength in the cores.

The requirement of a monoenergetic electron beam leads to the necessity of maintaining a linear variation of the induction over the working portion of the pulse length τ_p. In this case Eq. (1) takes the form

$$E_0 = -(N/\mathscr{L})\, S\Delta B/\tau_p, \qquad (3)$$

FIG. 2. The LIA-3000 accelerator. The beam energy is 3 MeV and the current 200 A.

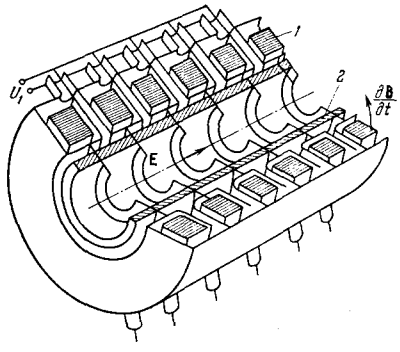

FIG. 3. Diagram of the induction system of an LIA. 1—ferromagnetic core, 2—accelerator tube.

where ΔB is the increase in the induction during the pulse length τ_p.

It can be shown that the energy transferred to the electron beam during the pulse is determined by the expression

$$W_1 = I_b \Delta B S N,$$

where I_b is the beam current.

It is evident that this energy is proportional to the change of flux in the core and does not depend on the duration of the pulse. For complete utilization of the core material, it is necessary before supplying the voltage pulse to the primary winding to transfer the core to the negative saturation region, which is almost always done[4,5]. This process is usually called reverse magnetization. The maximum current possible for the accelerated electrons in the presence of sufficient focusing to compensate space-charge repulsive forces is determined mainly by the power of the commutating element in the primary circuit, and at the present time the acceleration of a beam with a current of tens of kiloamperes appears realistic.

In principle the length of the accelerating voltage pulse in an LIA can be arbitrary. However, the increase of the core cross section with increasing pulse length beyond a few microseconds in accordance with Eq. (3) leads to a size of the induction system in which the weight of ferromagnetic material in the cores becomes unacceptably large. For a pulse length less than several tens of nanoseconds the energy loss in reversal of the core magnetization reaches a value at which the use of ferromagnetic materials in the accelerator is of little effect. For this region of pulse length, iron-free LIA can be used[22]. We can suggest that the range of pulse lengths for LIA with ferromagnetic cores lies in the range 20—700 nsec.

In LIA, as in high-frequency linear accelerators, the accelerating field is distributed along the entire accelerator and there is no gap to which a voltage corresponding to the total energy of the accelerated beam is applied. This makes unnecessary a cumbersome and dangerous compressed-gas installation and makes it possible to increase the final energy by simply increasing the number accelerating elements. On the other hand, the LIA preserves the advantages of transformers, allowing acceleration of beams with currents of hundreds or thousands of amperes with high efficiency, which cannot be done with high-frequency linear accelerators. In addition, as follows from Eq. (2), in LIA a beam can be obtained both with constant energy during the pulse and with an energy varying according to a previously specified law by providing a suitable shape of the primary voltage pulse.

3. THE ROTATIONAL ELECTRIC FIELD

It is well known that Maxwell's equations for a rotational electric field **E** and the magnetic field **H** produced by a constant current are similar. Therefore in determination of the accelerating electric field we can use the known solutions for the magnetic field of constant currents, replacing the current-density vector **j** by $\partial B/\partial t$.[24,25] However, in the working range of LIA there are always electrically conducting elements (the primary coil, the accelerator tube electrodes, and so forth), as a consequence of which it is necessary in an accurate calculation of the distribution of **E** to solve Laplace's equation with the appropriate boundary conditions determined by the design of the induction system.[4,25]

In the LIA-3000 induction system[5] a vacuum can be maintained without the use of an accelerator tube, and the specially formed electrodes constitute the primary windings. A diagram of this system and the field distribution on its inner boundary are shown in Fig. 4. In this case the solution of Laplace's equation for the field components will have the form[26]

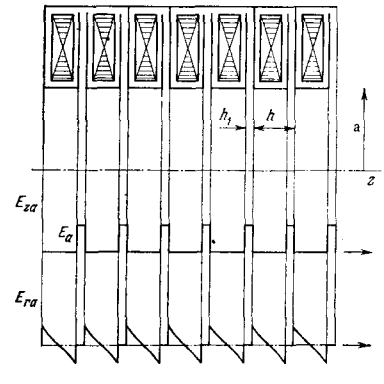

FIG. 4. Drawing and boundary conditions of the induction system for the LIA-3000.

$$E_z = A_1 I_0(k_1 r)\,[B_1 \cos(k_1 z) + C_1 \sin(k_1 z)], \quad (4)$$

$$E_r = A_2 I_1(k_2 r)\,[B_2 \cos(k_2 z) + C_2 \sin(k_2 z)]; \quad (5)$$

here $I_0(k_1 r)$ is a modified Bessel function of the first kind of zero order, $I_1(k_2 r)$ is a modified Bessel function of the first kind of first order, and $A_{1,2}$, $B_{1,2}$, $C_{1,2}$, and $k_{1,2}$ are constants determined by the boundary conditions.

The boundary conditions are a periodic function which can be expanded in Fourier series and hence can be written in the form

$$E_{z,a} = \frac{\alpha_0}{2} + \sum_{n=1}^{m} \alpha_n \cos\left(n\frac{2\pi}{T} z\right) + \sum_{n=1}^{m} \beta_n \sin\left(n\frac{2\pi}{T} z\right), \quad (6)$$

$$E_{r,a} = \frac{\gamma_0}{2} + \sum_{n=1}^{m} \gamma_n \cos\left(n\frac{2\pi}{T} z\right) + \sum_{n=1}^{m} \delta_n \sin\left(n\frac{2\pi}{T} z\right). \quad (7)$$

For the boundary conditions we have

$$E_{z,a} = 0 \quad \text{for} \quad 0 \leqslant z < (h - h_1)/2, \quad (8)$$

$$E_{z,a} = E_a \quad \text{for} \quad (h - h_1)/2 < z \leqslant h/2. \quad (9)$$

Determining the constants in Eq. (4) by means of Eqs. (6)—(9), we obtain an expression for E_z

$$E_z = \eta E_a \left[1 + \sum_{n=1}^{m} E_n I_0\left(n\frac{2\pi}{h} r\right) \cos\left(n\frac{2\pi}{h} z\right)\right], \quad (10)$$

where

$$E_n = (-1)^n 4 \cos\left(n\frac{\pi}{2}\eta\right) \sin\left(n\frac{\pi}{2}\eta\right) \Big/ \pi\eta n I_0\left(n\frac{2\pi}{h} a\right),$$

$$\eta = h_1/h.$$

It is easy to see that

$$\eta E_a = U_1/h = E_0.$$

Then Eq. (10) is written in the form

$$E_z = E_0 \left[1 + \sum_{n=1}^{m} E_n I_0\left(n\frac{2\pi}{h} r\right) \cos\left(n\frac{2\pi}{h} z\right)\right]. \quad (11)$$

The quantity $I_0(n2\pi a/h)$ increases rapidly with increasing n, and therefore in a rather large region of great interest we can limit ourselves to the first term of the series and retain sufficient accuracy.

The ratio of the amplitude of the first harmonic to the constant component is shown for illustration in Fig. 5a for several values of a/h and h_1/h. It is evident that the ratio a/h is the principal important factor and that for a rather uniform field it is necessary to have $a/h > 1$. If we assume that the boundary function for the radial component is odd, and in the region where curl $\mathbf{E} = 0$ (which occurs inside the system),

$$\partial E_z/\partial r = \partial E_r/\partial z,$$

we obtain from Eqs. (5) and (7) an expression for the radial component

$$E_r = E_0 \sum_{n=1}^{m} E_n I_1\left(n\frac{2\pi}{h} r\right) \sin\left(n\frac{2\pi}{h} z\right). \quad (12)$$

The ratio of the first harmonic E_{r1} to E_0 is shown in Fig. 5b.

The expressions given were obtained without inclusion of the field distortion at the edge of the system. Analysis of the falloff of the field near the edge of the system[27] shows that at a distance from the boundary equal to three aperture diameters (~6a), the field on the axis is for practical purposes equal to E_0.

Analysis of a system with an accelerator tube and

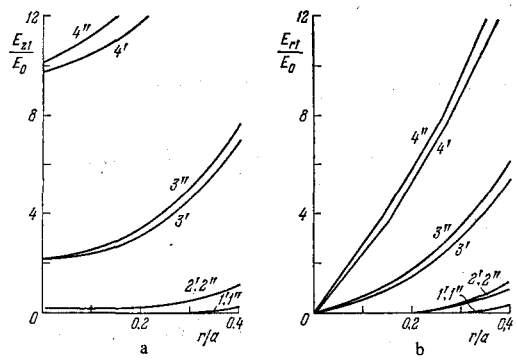

FIG. 5. Ratio of first-harmonic amplitude to constant component (%). a) Axial component; b) radial component. a/h = 2(1), 1.5 (2), 1 (3), and 0.75 (4); h_1/h = 1/4 (1′–4′) and 1/8 (1″–4″).

electrodes in the form of disks (Fig. 3) gives an expression for the field of form[4,25]

$$E_z = E_0 \left\{1 + \sum_{n=1}^{m} \alpha_n \left[I_0\left(n\frac{2\pi}{h} r\right) \Big/ I_0\left(n\frac{2\pi}{h} a\right)\right] \cos\left(n\frac{2\pi}{h} z\right)\right\}, \quad (11a)$$

$$E_r = \sum_{n=1}^{m} \delta_n \left[I_1\left(n\frac{2\pi}{h} r\right) \Big/ I_1\left(n\frac{2\pi}{h} a\right)\right] \sin\left(n\frac{2\pi}{h} z\right)\Big\}, \quad (12a)$$

where α_n and δ_n are determined by the conditions at the boundary. As in the preceding case, the field uniformity is determined to a significant degree by the ratio a/h, where a is the diameter of the opening in the electrodes and h is the distance between them.

If necessary the field uniformity can be improved by introducing a conducting cylinder into the working region[28,29]. At the time of the pulse a current

$$j_a = \varepsilon \partial \mathbf{E}_a/\partial t + \sigma \mathbf{E}_a$$

will flow along the cylinder. If $|\epsilon \partial \mathbf{E}_a/\partial t| \ll |\sigma \mathbf{E}_a|$, which is well satisfied in the range of pulse lengths characteristic of LIA, then

$$j_a = \sigma E_a. \quad (13)$$

From Eq. (13) and the equation of charge continuity it follows that for σ = const, $\mathbf{E}_a$ = const. This condition is fulfilled by the requirement $\eta = 1$ in Eq. (10), from which it follows that the amplitude of the harmonics is equal to zero over the entire region inside the cylinder. The value of the electrical conductivity is chosen on the basis of a number of conditions[29], for example, for the planned installation LIA-30/250[12] the surface conductivity is in the range 10^{-4}—10^{-3} ohms^{-1}. The conducting cylinder can be made from a vacuum-tight ceramic with a conducting layer deposited on its inner surface and replaces the sectionalized accelerator tube used in presently operating accelerators[4,5].

4. ACCELERATING SYSTEM

The accelerating system of an LIA consists of the induction system together with the system for producing the rectangular pulse of accelerating voltage. However, the term accelerating system is sometimes used to mean only the induction system. This is not quite accurate, since the induction system is one of the elements of a single high-current circuit, all elements of which affect the shape and magnitude of the accelerating voltage pulse, particularly in the nanosecond region. In Fig. 6 we have shown a simplified diagram of an accelerating system, which has been arbitrarily divided into

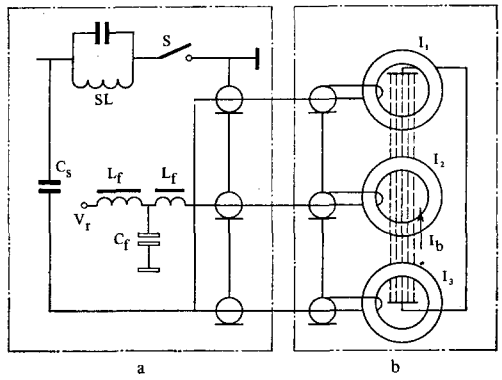

FIG. 6. Simplified diagram of accelerating system. a) Pulse system; b) induction system; SL—shaping line, S—switch, C_s—storage capacitance, V_r—reverse magnetization voltage, C_f—filter capacitor, L_f—filter inductance, $I_{1,2,3}$—inductors, I_b—beam current.

an induction system and a pulse-shaping system or, in other words, a pulse system.

Although the induction system of an LIA is qualitatively a set of single-turn pulse transformers, use of the calculation methods used in design of pulse transformers working in the microsecond region[30-32] turns out to be unsatisfactory, particularly with use of ferromagnetic materials with a rectangular hysteresis loop[33,34]. This is true for the following reasons.

In the first place, pulse transformer theory considers processes in cores made of electrical steel characterized by a nearly linear dependence of ΔB on H.[30] Comparative experiments have shown that higher efficiencies can be obtained in LIA with use of precision magnetically soft alloys with a narrow, nearly rectangular hysteresis loop. In particular, the iron-nickel alloy 50NP has been used in operating accelerators[4,5]. The magnetization reversal processes for these alloys have distinctive features[35]. For an accelerating voltage pulse length of tens of nanoseconds, it is possible to use magnetically soft ferrites[23,28]. Study of their magnetization reversal characteristics has shown that ferrites of the manganese-zinc group have characteristics which are close in shape to the characteristics of alloys with a rectangular hysteresis loop.

In the second place, for the pulse lengths of tens and hundreds of nanoseconds which are characteristic of LIA, the thickness of the tape from which the cores are prepared is chosen in the interval 10—20 μ. For this thickness the effect of eddy currents is comparable with the magnetic hysteresis[35], which is not taken into account in pulse-transformer theory. Reversal of the magnetization of a core of ferromagnetic material with a rectangular hysteresis loop with inclusion of the effects of eddy currents and hysteresis has been studied by a number of authors, for example refs. 35—37, and for practical purposes is described by the equation

$$H(t) = H_0 + g(B)\, dB/dt; \tag{14}$$

here H_0 is the initial field, whose value depends on the kind of material and is several times greater than the coercive force;

$$g(B) = (\sigma d^2/8B_r)(B + B_r) + [R_m(1 - B^2B_s^{-2})]^{-1}, \tag{15}$$

where B_r and B_s are the residual induction and saturation induction, d is the thickness of tape from which the core is wound, σ is the electrical conductivity of the ferromagnetic material, and R_m is a constant with dimensions of ohms/m; R_m depends on the kind of material. The first term in the right-hand side characterizes the effect of eddy currents, and for ferrites it is zero. The second term is due to hysteresis and occurs both for ferrites and for metallic ferromagnets.

Calculations and experiments show that for metallic cores the first term can be neglected for a tape thickness less than 5 μ, and the second for a tape thickness greater than 30—40 μ. In LIA, tape thicknesses of 10—20 μ are used, since use of tape thinner than 5 μ is technically difficult and comparatively expensive. For tape thicknesses greater than 20 μ the efficiency drops and the utilization of the material is poorer[38].

Integrating Eq. (14) with respect to time, we obtain

$$\int_0^t [H(t) - H_0]\, dt = \int_{B_{\text{init}}}^{B(t)} g(B)\, dB. \tag{16}$$

The integral on the left side is called the field impulse, and for complete magnetization reversal its value does not depend on the duration and shape of the reverse magnetization voltage and current, since

$$\int_0^\tau [H(t) - H_0]\, dt = \int_{-B_s}^{+B_s} g(B)\, dB = g_1(+B_s) - g_1(-B_s) = S_\omega,$$

where τ is the pulse length for complete reverse magnetization. The field impulse for complete magnetization reversal is called the switching coefficient and represents the quantity of electricity per unit core length necessary for complete magnetization reversal.

After integration of Eq. (16) with inclusion of (15) we obtain an expression for the field impulse

$$\int_{B_{\text{init}}=-B_r}^{B(t)} g(B)\, dB = \frac{\sigma d^2}{16B_r}[B(t) + B_r]^2 + \frac{B_s}{R_m}\left[\operatorname{arcth}\frac{B_r}{B_s} + \operatorname{arcth}\frac{B(t)}{B_s}\right]. \tag{17}$$

The slope of the magnetization reversal curves changes sharply at $B > 0.75B_s$. Therefore it is usually desirable to reverse magnetize the core to $B > B_r$. If we take into account that in the interval $-B_r \le B \le B_r$ the arc tangent can be considered approximately linear, we find from Eq. (17) that the field impulse is

$$Q(\lambda) \approx (B_r\sigma d^2/4)\,\lambda^2 + (2B_s/R_m)\operatorname{arcth}(B_r/B_s)\cdot\lambda,$$

where $\lambda = \Delta B(t)/2B_r$. For $\lambda = 1$ it follows from Eq. (17) that

$$S_\omega = S_{\omega e} + S_{\omega 0},$$

where $S_{\omega e}$ is the component of the switching coefficient due to the action of eddy currents, and $S_{\omega 0}$ is due to the effect of hysteresis. Then,

$$Q(\lambda) = S_{\omega e}\lambda^2 + S_{\omega 0}\lambda. \tag{18}$$

After differentiating Eq. (18) with respect to t, taking into account that for a rectangular voltage pulse $d\lambda/dt = 1/\tau$, we obtain

$$H(t) = H_0 + (S_{\omega 0}/\tau) + (S_{\omega e}/B_r)(\Delta B(t)/\tau). \tag{19}$$

It is evident that within the accuracy of the assumptions made the dynamic hysteresis loop is broadened as a result of the initial field and hysteresis and has a slope due to eddy currents. In Table I we have given calculated values of $S_{\omega e}$ for the most common materials[39]. In Table II we have shown also the measured values of the total switching coefficient[35].

The real magnetization reversal curve differs somewhat from Eq. (19), and accurate values of the reversal

TABLE I. Switching coefficient $S_{\omega e}$ (μC/m) for a number of alloys

		E, EA, EAA	65NP	45NP, 50NP	79NM, 79NMA	80NKhS	42NS	38NS, 50NKhS	Carbonyl iron	
Electrical conductivity, 10^{-6} mhos/m		10	4	2,22	1.8	1.58	1,17	1.17	0.18	
Change in induction, T		4	2.5	2.8	1,4	1.3	1.8	1.8	0.5	
Tape thickness, μ	3	50	10	10	—	—	—	—	—	$S_{\omega e}$
	5	130	30	20	10	10	10	10	—	
	10	500	130	80	30	30	30	30	—	
	20	2 000	500	310	130	100	110	100	—	
	30	4 500	1 130	700	280	230	240	230	10	
	50	12 500	3 120	1940	790	640	660	630	30	
	100	50 000	12 500	7780	3150	2550	2630	2500	110	

TABLE II. Characteristics of most used magnetically soft materials

Type of alloy	Tape thickness d, μ	Residual induction B_r, T	Coercive force H_c, A/m	Start field H_0, A/m	Total switching coefficient S_ω, μC/m
50NP	5	1.4	40	110 — 120	110
	10	1.4	28	75 — 100	160
	20	1.3	20	55	330
34NKMP	5	1.5	24	145	80
	10	1.45	16	130	145
79NM	3	0.7	12	24	32
	5	0.8	8	20	48
	10	—	—	40	40

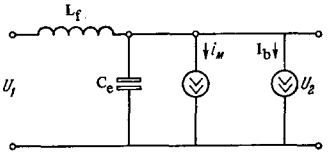

FIG. 7. Equivalent circuit of inductor.

field must be found from the experimental characteristics[40,41]. The nonlinear form of the magnetization reversal characteristic complicates the analytic discussion of processes in the induction system. The equivalent circuit of the induction system element (inductor) is shown in Fig. 7.[34] The circuit contains a magnetization current generator i_M,

$$i_M(t) = \pi D_{av} H(t). \tag{20}$$

The effect of the distributed capacitance between the inductors, i.e., essentially between the primary and secondary windings, and between the core and the primary winding is taken into account by introduction of an equivalent capacitance C_e into the circuit. The presence of the fringing flux between the windings is taken into account by inserting in the circuit a fringing inductance L_f. The effect of the winding resistance can usually be neglected in LIA, and it is not included in the circuit. The current of the charged particle beam can be represented by the current generator I_b, whose value is in general constant only during the flat part of the pulse and changes during the rise and fall. For rough calculations for pulse lengths $\tau_p \geq 0.5$ μsec it is possible to use the equivalent circuit method as customary for pulse transformers[42,43].

The energy loss in the core is determined by the integral

$$W_M = \int_0^t u i_M \, dt. \tag{21}$$

From Eq. (21) with inclusion of Eqs. (14) and (20) we obtain

$$W_M = VH_0\Delta B + (2VB_s/\tau_p)(S_{\omega 0}\lambda^2 + S_{\omega e}\lambda^3).$$

The quantity

$$W_{M,0} = VH_0\Delta B$$

is proportional to the energy stored in the core, which in general can be used repeatedly; however, this is not yet done in LIA. Here V is the core volume; it is assumed that the material has a rectangular hysteresis loop and that $B_r \approx B_s$.

The second term

$$W_{M,d} = (2VB_s/\tau_p)(S_{\omega 0}\lambda^2 + S_{\omega e}\lambda^3)$$

is the dynamic loss to eddy currents and hysteresis. For $\tau_p < 0.3$ μsec and for the materials usually used in LIA, the quantity $W_{M,0}$ can be neglected in comparison with $W_{M,d}$.

The quantity $W_{M,d}$ is always proportional to the core volume and inversely proportional to the magnetization reversal time. The dependence on the induction change ΔB is more complicated and is determined by the relation between $S_{\omega 0}$ and $S_{\omega e}$. The quantity $S_{\omega 0}$ is characteristic of the material itself and does not depend on the thickness of rolling. The quantity $S_{\omega e}$ is proportional to the square of the tape thickness. For a small tape thickness < 5 μ ($S_{\omega e} \ll S_{\omega 0}$), and also for ferrites, the quantity $W_{M,d}$ is proportional to ΔB^2. If eddy current losses dominate ($S_{\omega e} \gg S_{\omega 0}$), the energy loss is proportional to ΔB^3.

In view of the fact that the loss in the core is proportional to its volume and that the acceleration given to the particles is proportional to its cross-sectional area, it is advantageous, when it is necessary to obtain high efficiency and small weight of the accelerator, to minimize the core diameter and increase its axial length[24].

The quantity $W_b/(W_b + W_{M,0} + W_{M,d})$, which represents the ratio of the energy transferred to the beam to the total energy expended in reverse magnetization of the cores, is the principal component of the overall efficiency of the accelerator. Existing experimental data[40,41] permit this quantity to be estimated. It has values 0.12, 0.6, and 0.95 for a pulse length of 500 nsec and respective beam currents of 100, 1000, and 10 000 A

with tape of 50NP alloy 0.01 mm thick. For a pulse length of 50 nsec and the same current values the ratio is 0.02, 0.15, and 0.6, respectively.

The efficiency of LIA increases with increasing pulse length and accelerated beam current. The latter fact permits high efficiency to be obtained even for short pulse lengths. It is necessary to consider the fact that the average power in the beam of LIA reaches hundreds of kilowatts, and to retain the high efficiency provided by the induction system, it is necessary to approach complete transfer of the energy stored in the capacitor to the induction system. Laboratory installations form an exception to this statement[23]. Optimal transfer of energy to the pulse system is accomplished either by use of nonuniform artificial lines[13,44], whose theory has been developed by Litvinenko and Soshnikov[45], or by uniform lines in combination with a correction system[46]. The reliability of these systems is determined to a significant degree by the quality of the capacitors used. Paper-film pulse capacitors, which have a high reliability in operation with pulse-forming lines, are highly recommended.

The commutators are spark gaps[15,20] or hydrogen thyratrons[13,44,46]. The main deficiency of a spark gap is its limited life. Spark gaps usually lose their usefulness after 10^4—10^6 discharges. A system with a spark gap can be used in laboratory installations operating in the single-pulse mode. Pulsed hydrogen thyratrons are a reliable and long-lived device which have a high stability in their parameters and permit switching of currents of 10—15 kA at a high pulse repetition frequency. They are preferred in accelerators with a pulse length greater than 100 nsec. For pulse lengths of tens of nanoseconds it is necessary to have in mind that, as experiments have shown, the switching time of hydrogen thyratrons amounts to 30—50 nsec and it is necessary in the pulse system to provide elements for peaking the pulse. One possible solution is based on use of the properties of electromagnetic shock waves[23,47]. Shock waves arise in propagation of electromagnetic waves in a medium whose magnetic properties and, in particular, magnetic permeability, depend on the field strength H of the propagated wave. A suitable material for this purpose is a ferrite in which the permeability drops with increasing H and, consequently, the peak of the pulse is propagated with a higher velocity than the base. In this way the rise time of the pulse can be made less than 10^{-9} sec; however, such short rise times are difficult to achieve, since the presence of parasitic L_f and C_e in the induction system does not permit them to be made shorter than 5—10 nsec[34].

As was indicated above, the cores are transferred to a state of negative saturation by means of a magnetization reversal system. For materials with a rectangular hysteresis loop, after the core has been transferred to a state of saturation, the demagnetizing field can be reduced to zero. This corresponds to use of a reverse current pulse[4] for reverse magnetization.

In particular, use of a half sine wave[5] is possible. With materials of low rectangularity, for example, ferrites of the nickel-zinc group, before the main pulse is supplied the core must be subjected to a demagnetizing field in order to have the greatest increase in induction.

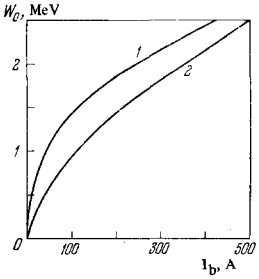

FIG. 8. Relation between current and initial energy of electron beam at which the beam increases its diameter by 1.5 times in 100 cm. r_b cm; 1—no accelerating field, 2—accelerating field of 10 kV/cm.

5. TRANSVERSE CONTAINMENT OF THE BEAM

Without an effective solution of the problem of limiting the radial size of the beam, reliable operation of LIA, particularly at pulse repetition frequencies of several hertz or higher, is impossible.

Thus, in LIA-30[13] the beam energy in each pulse will be 4 kJ, and naturally at a frequency of 50 Hz a beam loss of even a few percent can not only destroy the parts of the accelerator adjacent to the beam but also can produce inadmissibly intense activation of these parts (the electron energy at the output is 30 MeV).

The main difficulty in containment lies in the strong Coulomb repulsion of an intense electron beam. Figure 8 shows the relation between the beam current and initial energy for which a beam of diameter 3 cm increases its size by 1.5 times in a distance of 100 cm.[48]

In addition to space-charge forces, the beam is acted on by the Earth's field in the gaps between the elements of the induction system[49] and by the fringing fields.

In the accelerator for Astron the problem of size limitation and positioning of the beam is solved by use of short magnetic solenoids, placed between the accelerator sections and having comparatively large aperture (from 150 to 500 mm), in combination with a system of correcting coils[50]. In this system the best beam transmission was 90%, and 75% was considered satisfactory.

In redesign of the accelerator to increase the accelerated beam current to 1000 A, the length of the accelerating sections was shortened by a factor of two, i.e., to 50 cm, and 29 focusing solenoids and 9 correcting magnets were installed along the beam line. Beam position sensors and current monitors were also installed. The placement of the solenoids and correcting magnets was determined by computer calculation. In the calculation it was assumed that a magnetic field of 0.45×10^{-4} T existed along the beam line.[51] However, when this accelerator was put into operation it was found that beam currents greater than 500 A could not be obtained, as the result of instabilities which arose[17]. As a result the possibility was investigated of the appearance of instabilities due to generation of a high-frequency electromagnetic field and the interaction of the beam with image charges and currents. Neil and Cooper[52] show that intense electron beams excite an electromagnetic wave which has a magnetic field component transverse to the axis. Under the action of this field the beam is deflected from the accelerator axis and hits the chamber wall. Woods[53] has developed a theory of the interaction of a high current electron beam with image charges and currents. The image force has the form

$$F_{im} = q\,(2I_b/\beta^2 a)\,r,$$

where $q = [1 - (a/a_*)^2\beta^2]$, a is the internal radius of the beam—pipe electrodes, and a_* is the internal radius of the inductor core.

Inclusion of the image force in calculation of the dynamics of high-current beam leads to additional conditions imposed on the distance between lenses and the ratio between the size of the beam and that of the induction system. In particular, Woods[53] shows that the beam-pipe aperture should be 4—8 times the beam size.

The problem of containing the beam size is made easier by use of a continuous axially symmetric magnetic field[54]. Under the action of a magnetic field perpendicular to the axis, the beam is deflected by an amount Δr_1 determined by the expression[29]

$$\Delta r_1 = B\mathcal{L}^2/m_0 c\gamma, \tag{22}$$

where $\mathcal{L}$ is the distance at which the beam deflection is determined, and $\gamma = (1-\beta^2)^{-1/2}$. In the case where the beam passes through a continuous longitudinal magnetic field, the presence of a field component perpendicular to the axis leads to an inclination of the axis, and the deflection of the beam from the accelerator axis will be determined by the expression

$$\Delta r_2 = B\mathcal{L}/B\varphi, \tag{23}$$

where B_f is the field necessary for focusing the beam[54]

$$B_f = (m_0/r_b)\,(2I_b/\pi\varepsilon_0 ep)^{1/2}; \tag{24}$$

here p is the momentum of the electrons in the beam and r_b is the equilibrium radius of the beam. From Eqs. (22)—(24) we obtain

$$\Delta r_2/\Delta r_1 = 46\,(r_b/\mathcal{L})\,\gamma^{3/2}/I_b^{1/2}. \tag{25}$$

Analysis of Eq. (25) shows that in the initial part of the acceleration, which is most important from the point of view of containing the beam size, the limiting current in a system with a continuous field is 5—10 times higher than in a system using short solenoids. Estimates show also that in the case of a longitudinal magnetic field the deflection of the beam by image charges and currents is reduced.

The equation determining the shape of an accelerated axially symmetric beam in a longitudinal magnetic field in the period following the working portion of the pulse has the form[54]

$$p\,(m_0^2c^2+p^2)\,\frac{d^2r}{dp^2}+p^2\,\frac{dr}{dp}+\frac{1}{2}\,r\left(\frac{Bc}{E}\right)^2 p=\frac{I_b m_0^2 c^2}{2\pi\varepsilon_0 e E^2}\,\frac{1}{r}. \tag{26}$$

In derivation of this equation it is assumed that the potential due to the space charge of the beam does not affect the longitudinal motion of the particles, that the accelerating field has only a longitudinal component, that the magnetic field at the cathode is zero (Brillouin flow), that the beam is laminar, that the paraxial conditions are satisfied, and that effects occurring in the rise and fall of the pulse can be ignored. If the field at the cathode is not zero, then a term appears in Eq. (26) due to the initial magnetization of the beam[55]. In LIA the magnetic field at the cathode is usually zero. Since the size is smallest in this case, we will use the equation in the form of (26) in the subsequent discussion. The term on the right-hand side of Eq. (26) corresponds to the repulsive force, and the last term on the left-hand side to the force attracting the beam to the axis. Since the force which produces the spreading of the beam is inversely proportional to the radius and the force attracting the beam is directly proportional to the radius, for each p(z) there should exist an equilibrium value $r = r_1(p)$ for which the force acting on a peripheral particle of the beam is zero. From Eq. (26) we have the following expression for this equilibrium trajectory:

$$r_1(p) = (m_0/B_f)\,(2I_b/\pi\varepsilon_0 ep)^{1/2}.$$

If a peripheral electron is in an equilibrium trajectory, its radius falls monotonically, inversely as the square root of p. For small departures of the initial conditions from equilibrium, the beam experiences pulsations whose period increases as the energy increases. For the magnitude of the pulsations to remain small, the necessary condition is

$$2\,(Bc/E)^2 \gg 1.$$

Since the repulsive space-charge force falls off as $1/\gamma^2$, for a beam energy of 3—5 MeV it is no longer necessary to use a continuous magnetic field and the radial dimensions of the beam can be contained by means of short magnetic solenoids located between the sections of the induction system[56]. The location of the solenoids is determined by numerical solution of Eq. (26) in the regions between two neighboring solenoids for various values of beam convergence. By means of such a calculation a trajectory is chosen with a ratio r_{max}/r_{min} corresponding to stable motion of the beam with respect to departures of its initial parameters from the equilibrium values[57]. Analysis of the behavior of the beam for deviations of the focusing-system parameters from the nominal values shows that the tolerances on deviation of the parameters are not severe[56].

As was noted above, in the studies cited the analysis of beam dynamics is carried out on the assumption of laminar electron flow and paraxial conditions. This assumption is valid to a sufficient degree for an equilibrium distribution of the charge density over the beam cross section. Experimental study of the parameters of an electron beam accelerated in an LIA shows that the charge density distribution over the cross section can be nonequilibrium[58]. The Coulomb repulsive force and the combined force acting on the electrons in this case are appreciably nonlinear. This nonlinearity leads to crossing of trajectories and to formation of a nonlaminar (multivelocity) structure of the electron flow. Analysis of nonlinear electron flow shows that the distribution of charge density over the beam cross section does not remain constant at different points along the beam and that the maximum charge density can occur at the boundary of the beam[59].

A possible means of decreasing the effect of the space charge of a beam accelerated in an LIA is to compensate it by residual gas ions. For a residual gas pressure less than 10^{-3} Torr the compensation time is greater than the accelerating voltage pulse length, which results in the necessity of preliminary ionization of the residual gas, for example, by an electron beam[28] or a high-frequency field[19].

Recent investigations of a plasma betatron[60] show that during acceleration beam-plasma interactions arise which lead to loss of a third of the beam energy and to broadening of the energy spectrum of the accelerated electrons. However, in spite of these difficulties, the current reaches 1000 A even at the low energy of 40 keV. Use of a plasma with a falloff in its density along the accelerator length results in a sharp decrease in the efficiency of the beam-plasma interaction. The beam loss decreases and the electron energy spectrum becomes narrower.

TABLE III. Parameters of linear induction accelerators

Name of accelerator	Location	Beam energy, MeV	Beam current, A	Length of flat part of pulse, nsec	Repetition frequency, pulses/sec	Energy spread, %	Emittance, πcm-mrad
Astron injector before reconstruction[4,17]	Livermore, USA	3.7	350	300	0—60 (5)	<3	50
LIA-3000 [5]	Dubna, USSR	3 (1.8)	200	350	0—25 (<1)	—	—
Astron injector after reconstruction [17,51]	Livermore, USA	4.2	800	300	0—60 (5)	<2	25
LIA-30/250 (under construction) [12,13]	Dubna, USSR	30	250	500	0—50	<3	—
ERA injector [14,15,61]	Berkeley, USA	4.25	500	45	<1	<0.5	<70
SILUND (under construction) [22]	Dubna, USSR	3	2000	20	0 — 50	<2	—
Plasma betatron [19,20,60]	Khar'kov, USSR	0.05—0.1	500—1000	—	Single	Broad spectrum	—
Iron-free LIA [22]	Moscow, USSR	2	2000	70 (half sine wave)	»	—	—

6. ACCELERATOR PARAMETERS. DESIGN OF THE MAIN SYSTEMS

The main parameters of LIA which are operating or under construction are given in Table III. The values at which the accelerator usually operates are shown in parentheses. In addition to these accelerators, several installations are in the planning stage. Except for the plasma betatron, all of the installations serve as injectors, and beam quality is of primary importance. The plasma betatron is a research laboratory installation intended for study of the acceleration of an electron beam in plasma. All of the installations listed in Table III are characterized by peak beam currents 2—3 orders of magnitude greater than the currents in traveling-wave linear electron accelerators[62]. With the existing level of technology we can expect that the current accelerated in LIA can be increased to tens of kiloamperes. Most existing LIA are intended for study of the new collective method of acceleration, and their energy is determined by this problem.

However, accelerators with substantially higher energies appear quite realistic. For example, a 30-MeV accelerator[13] is under construction. An LIA is being discussed for acceleration of an electron ring to 1.6 BeV. The average accelerating field strength is 5 MeV/m and the length is 320 m.[15] The maximum pulse repetition frequency is still small. It is determined by the quality of the beam guidance along the accelerator and by the characteristics of the switching elements in the pulse supply system. In principle, a frequency of 1000 pulses/sec can be reached with use of contemporary pulsed hydrogen thyratrons.

An advantage of LIA is the possibility of obtaining beams with high quality. The energy spread can be made less than 0.5%, as the result of the video-pulse mode of operation of the accelerator. Here the beam has a low emittance. High efficiency in combination with simplicity in use and reliability over a wide range of variation of the parameters of the surroundings makes the use of these accelerators extremely promising also in industry and geology.

The induction system usually incorporates cores of ferromagnetic material, which permits a significant reduction in the current in the primary winding of the inductors in comparison with so-called iron-free accelerators. For example, for cores made of 50 NP alloy tape of thickness 20 and 10 μ, the average value of

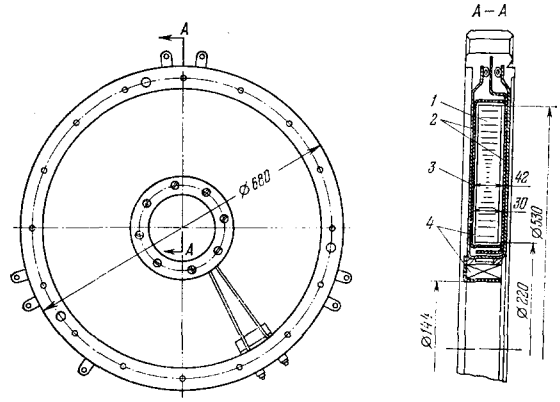

FIG. 9. Design of LIA-3000 inductor (dimensions in mm). 1—core, 2—insulating jackets, 3—primary winding, 4—focusing coil.

$\mu = \Delta B/\mu_0 H$ is respectively 2000 and 4000 for a pulse duration $\tau_{0.95} = 0.5$ μsec.[63] This in turn provides the possibility of raising the efficiency of the accelerator to the high values mentioned earlier.

The induction system is made of sections whose dimensions are determined by the requirements on the focusing system, the vacuum system, and purely design considerations. In the spaces between the sections are located focusing lenses, pumping leads, and arrays of diagnostic apparatus.

The sections in turn consist of a series of identical elements (inductors). Figure 9 shows the design of an inductor for the LIA-3000 accelerator[5]. The inductor core is wound on a special lathe, and at the same time magnesium oxide insulation is deposited by cataphoresis. After winding, the core is heated in a vacuum furnace and then covered with an insulating jacket of mica. The insulating jacket and a layer of rubber provide the necessary electrical insulation of the core and also protect it from mechanical and thermal stresses, which facilitates retention of the magnetic characteristics during construction, shipping, and use of the inductor.

The exciting winding is made in the form of a torus of rectangular cross section (in the shape of the core). All parts of the inductor are assembled with an epoxy resin of special composition. The inductor design provides the possibility of constructing an accelerator without a vacuum pipe[64]. A somewhat different inductor design is proposed for use in the LIA-30/250 accelerator. A

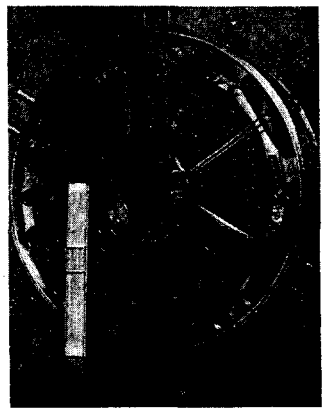

FIG. 10. Photograph of LIA-30/250 inductor.

photograph of this inductor is shown in Fig. 10.[13] This inductor is required to operate under conditions of intense neutron radiation and is made without use of epoxy resin; the only insulating material used is a mica preparation which has high stability under radiation. In addition, the core is made of two halves enclosed in mica insulating jackets. The two halves are clamped to a watercooled housing. In this way the voltage between the primary winding turns and the core is reduced to half the primary voltage, which obviously decreases the insulation requirements, and the heat flow from the core is directly to the housing, bypassing the insulation, which also eases the operating conditions.

Figure 11 shows a cross section of a section of the Astron injector after reconstruction[17]. It consists of set of cores enclosed by the primary and secondary turns. Inside the section is mounted a sectionalized accelerator tube, between whose electrodes the accelerating field exists, and inside this tube is maintained the vacuum necessary for existence of the beam, usually $10^{-6}-10^{-5}$ Torr.

As a result of the relatively short duration of the accelerating voltage pulse in the accelerator SILUND, it was found possible to use type 300 NN ferrite[23] for the cores. In this case the section is also made up of inductors; however, since the ferrite is a dielectric, there is no need of special insulation between the turns and the core.

The sections of the injector for the Electron Ring Accelerator are also made with specially selected ferrites, but the design of these sections is quite different[61]. A cross section of this section is shown in Fig. 12. In essence, the section in this case consists of one inductor with a voltage of 250 keV on the accelerating gap. The inside of the inductor is filled with ferrite and transformer oil, which provides the necessary electrical stability. The pulse-forming line is connected directly to the section. With this design there is no need of a special accelerator tube and the impedance of the system is raised considerably, which facilitates the shaping of the pulse.

However, the difficulties resulting from increased voltage become greater and, naturally, the reliability of the operation of the induction system is reduced. Furthermore, a pulsed hydrogen thyratron cannot be used as the switching element in the pulse system, since the anode voltage of developed thyratrons does not exceed 80 kV, and it is necessary to use a spark gap; consequently, operation is limited to single pulses. The pulse system is a double line of the Blumlein type with an air

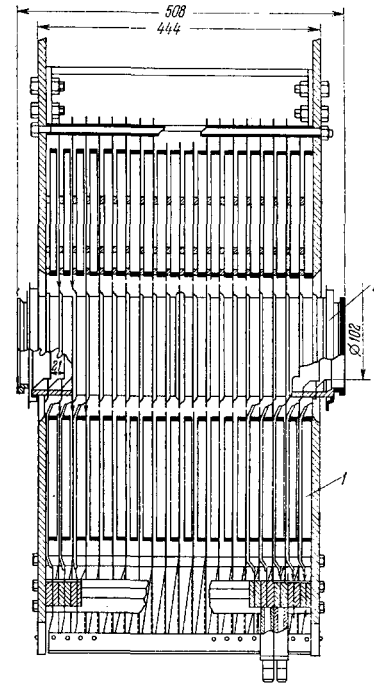

FIG. 11

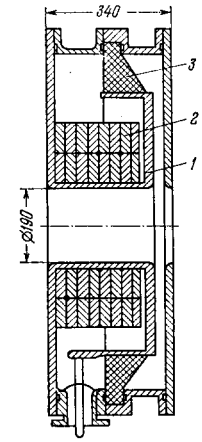

FIG. 12

FIG. 11. Cross section of a section of the Astron injector (dimensions in mm). 1—core, 2—accelerating tube.

FIG. 12. Cross section of a section of the injector for the Electron Ring Accelerator (dimensions in mm). 1—primary winding, 2—core, 3—insulating plate.

spark gap as switching element. The interior of the line is filled with transformer oil. The feedthrough insulators between the air spark gap (pressure 10 atm) and the oil-filled line are made of epoxy resin. The line is charged from a Marx generator in a time of 330 nsec. The line voltage is now close to the breakdown for the spark gap, and if the gap is not specially triggered it will break down spontaneously after 100 nsec. This mode of operation of the spark gap assures a small spread in the firing time, ~1 nsec. Direct connection of the forming line to the accelerating section and use of an air spark gap under pressure permits a rather short rise time of 12 nsec to be obtained for the accelerating voltage pulse.

In another nanosecond accelerator of the SILUND tubes are type TGI-1-3000/50 hydrogen thyratrons. Experience shows that pulsed hydrogen thyratrons for pulse lengths less than 1 μsec can switch currents several times larger than their rated values[46,65]. However, the switching time is several tens of nanoseconds. In order to reduce the rise time, a peaking system consisting of coaxial line with ferrite is installed between the capacitor bank and the inductor in this accelerator. Correction of the flat portion of the pulse is accomplished by choice of the value and sign of the initial magnetization of the ferrites in the correcting lines. In the system described it is possible to obtain a rise time of 5 nsec with a flat top of 20 nsec.

In the accelerators LIA-3000 and LIA-30/250 the pulse lengths are respectively 350 and 500 nsec, and use of pulsed hydrogen thyratrons does not require the addition of a peaking circuit. In shaping the flat portion of the pulse, use is made of a nonuniform line with lumped parameters[44], the variation of impedance being matched to that of the induction system.

When a longitudinal magnetic field is used to contain the beam size, coils are mounted along the internal diameter of the inductors, with leads brought out on one side of the inductor.

In addition to the elements discussed, an important part of the accelerator is the electron gun. Its design determines to a large extent the current value, beam quality, and reliability of operation of the accelerator. The high voltage power supplies for guns in LIA, as a rule, utilize pulse transformers made of the same elements as the induction system, i.e., of inductors.

In the Astron injector the pulse transformer is a section similar in design to the main sections but somewhat larger in diameter[4,17]. In the center of the section are located the gun electrodes, which are used to produce not only a longitudinal component but also a radial component of the electric field. In this way compensation of the repulsive space-charge forces is achieved. The required gradient distribution is achieved by choice of the distance between the electrodes and of the number of cores between successive electrodes. The accelerator gun, after reconstruction, has an oxide cathode in the shape of a flat disk 17.8 cm in diameter. The anode aperture is covered by a grid to avoid a drop in the electric field.

The entire apparatus is placed in a tank through which Freon flows at a pressure of 2 atm. This decreases corona and removes heat from the section. The gun provides a current of 1200 A at a voltage of 550 kV. This corresponds to a microperveance of 2.9.

In the LIA-30/250 accelerator the pulse transformer will consist of a section of the main accelerator along whose axis is placed a metal rod; the gap between the rod and the inductor housing is filled with transformer oil[13,66]. The voltage of 300 kV is taken out through a feedthrough insulator and fed to the cathode of the electron gun. A special cathode with 50-mm diameter and a high value of specific emission is used[57]. The gun current is >250 A.

In the injector of the Electron Ring Accelerator the pulse transformer consists of five sections mounted together[61]. Along the axis of the sections is placed a metal rod terminated in a spherical tip. The rod serves as a support. On the tip is placed a field-emission cathode made of tantalum tape 0.012 mm thick wound in a spiral with outer diameter 10 mm. The anode aperture is covered with a grid of 0.075-mm diameter tungsten wire with a 3-mm mesh. With a voltage of about 1 MV, a current of 1200 A is extracted from the gun. The cathode will withstand $(3-5) \times 10^5$ pulses without destruction. The other elements and systems of the LIA are similar to those of other accelerators and do not require special description.

7. CONCLUSION

During the 1960s there have been developed and built a number of LIA intended for carrying out research in the field of new methods of acceleration and controlled thermonuclear fusion. A large number of papers have been published on the physics and technology of accelerators of this type. It has been shown that beams with currents of hundreds or thousands of amperes can be accelerated in LIA with low energy spread and excellent emittance, which makes them extremely attractive to physics researchers.

In addition, LIA are reliable and simple to use, do not require special surroundings, and have high efficiency. This enables us to expect that, in addition to the ever increasing use of LIA in scientific research, they will be used also in industry. For example, LIA can form the basis of portable, cheap, and simple installations for x-ray structural analysis, γ-ray logging, and defectoscopy which are capable of operation under field and factory conditions.

[1] N. Christofilos, Nucl. Fusion Suppl., pt. 1, 159 (1962).
[2] V. I. Veksler, Atomnaya énergiya **2**, 427 (1957).
[3] W. A. S. Lamb, IRE Trans. Nucl. Sci. **NS-9**, 53 (1962).
[4] N. C. Christofilos et al., Rev. Sci. Instr. **35**, 886 (1964).
[5] A. I. Anatskiĭ et al., Atomnaya énergiya **21**, 439 (1966).
[6] A. Bowersy, Elektrische Hochspannugen, B., 1939.
[7] J. W. Beal et al., Plasma Physics and Controlled Nuclear Fusion Research, Conference Proceedings (Novosibirsk, August 1—7, 1968), v. 1, Vienna, IAEA, 1969.
[8] V. I. Veksler et al., Atomnaya energiya **24**, 317 (1968).
[9] V. P. Sarantsev, Vestn. AN SSSR (Bulletin, Academy of Sciences, USSR), No. 12, p. 54 (1968).
[10] V. I. Veksler et al., Proc. of the 6th Intern. Conf. on High Energy Accelerators, Cambridge, CEAL-2000, 1967, p. 289.
[11] V. P. Sarantsev et al., Preprint JINR R9-5558, Dubna, 1971.
[12] V. D. Anan;ev et al., Preprint JINR 13-4392, Dubna, 1969.
[13] A. I. Anatsky et al., IEEE Trans. Nucl. Sci. **NS-18**, No. 3, 625 (1971).
[14] D. Keefe, Part. Accel. **1**, 1 (1970).
[15] J. M. Peterson et al., Proc. Second All-Union Conf. on Charged Particle Accelerators, Moscow, November 11—18, 1970, v. 1, Moscow, Nauka, 1972.
[16] V. K. Grishin, Prib. Tekh. Éksp., No. 1, 35 (1970) [Instrum. Exp. Tech.].
[17] J. W. Beal et al., IEEE Trans. Nucl. Sci. **NS-16**, No. 3, 294 (1969).
[18] V. K. Grishin and V. G. Sukharevskiĭ, Vestn. MGU, Fizika, v. 25, p. 591 (1970) [Moscow University Physics Bulletin **25**, No. 5, p. 92].
[19] E. I. Lutsenko et al., Zh. Tekh. Fiz. **35**, 635 (1965) [Sov. Phys.-Tech. Phys. **10**, 499 (1965)].
[20] N. S. Pedenko et al., in Vzaimodeĭstvie puchkov zaryazhennykh chastits s plazmoĭ (Interaction of Charged Particle Beams with Plasma), Kiev, Naukova dumka, 1965.
[21] V. K. Grishin and V. G. Sukharevskiĭ, Vestn. MGU, Fizika, v. 25, p. 570 (1970) [Moscow University Physics Bulletin **25**, No. 5, p. 68].
[22] A. I. Pavlovskiĭ et al., Atomnaya énergiya **28**, 432 (1970) [Sov. Atomic Energy].
[23] V. D. Gitt et al., Preprint JINR R9-5601, Dubna, 1971.
[24] I. M. Matora, Preprint JINR R9-3184, Dubna, 1967.
[25] Yu. P. Vakhrushin and O. V. Semenov, Zh. Tekh. Fiz. **38**, 1521 (1968) [Sov. Phys.-Tech. Phys. **13**, 1238 (1969)].
[26] W. R. Smythe, Static and Dynamic Electricity, New York, McGraw-Hill, 1950. Russ. transl., Moscow, IL, 1954.
[27] Yu. P. Vakhrushin et al., Preprint, JINR 9-3287-2, Dubna, 1967.
[28] Yu. P. Vakhrushin, Candidate's dissertation, Research Institute of Electrophysical Apparatus, Leningrad, 1967.

[29] Yu. P. Vakhrushin and V. K. Gagen-Torn, Preprint, Research of Electrophysical Apparatus A-0123, Leningrad, 1971.
[30] R. V. Lukin, Radiotekhnika **2** (4), 46 (1947).
[31] Ya. S. Itskhoki, Impul'snye transformatory (Pulse Transformers), Moscow, Sov. radio, 1950.
[32] M. M. Aĭzinov, Perekhodnye protsessy v élementakh radioustroĭstv (Transition Processes in Radiofrequency Elements), Leningrad, Morskoĭ transport, 1955.
[33] É. F. Zaĭtsev, Radiotekhnika **23**, (6), 59 (1968) [Telecomm. Radio Engr.].
[34] L. A. Meierovich et al., Magnitnye generatory impul'sov (Magnetic Pulse Generators), Moscow, Sov. radio, 1968.
[35] A. I. Pirogov and Yu. M. Shamaev, Magnitnye serdechniki s pryamougol'noĭ petleĭ gisterezisa (Magnetic Cores with Rectangular Hysteresis Loops), Moscow, Énergiya, 1964.
[36] A. Goral, Bull de l'Ac. Polon. Sci., Ser. des Sci. techn. **8**, 297 (1960); Electron. Eng. **32**, 116 (1960).
[37] V. G. Mikhalev, Tr. MFTI (Proceedings, Moscow Physico-technical Institute), No. 8, p. 38 (1962).
[38] V. L. Dyatlov, Nauchn. dokl. vyssh shkoly (Élektromekhanika i avtomatika) (Scientific Reports of the University, Electromechanics and Automation), No. 2, 3 (1959).
[39] M. G. Vitkov, Avtomatika i telemekh. (Automation and Remote Control) **23**, 1686 (1962).
[40] N. P. Barshteĭn et al., Élektron. tekh. ser. 9, No. 3, 95 (1971).
[41] A. I. Anatskiĭ et al., Preprint, JINR R9-6075, Dubna, 1971.
[42] A. I. Anatskiĭ, et al., Élektrofiz. apparatura (Electrophysical Apparatus), Moscow, Atomizdat, No. 8, p. 134 (1969).
[43] P. V. Bukaev and V. P. Sarantsev, Preprint, JINR R9-5129, Dubna, 1970.
[44] A. I. Anatskiĭ, et al., Trudy Vsesoyuznogo soveshchaniya po uskoritelyam zaryazhennykh chastits (Proceedings All-Union Conf. on Charged Particle Accelerators), Moscow, October 9—16, 1968, v. 2, Moscow, Atomizdat, 1970.
[45] O. N. Litvinenko and V. I. Soshnikov, Teoriya neodnorodnykh liniĭ i ikh primenenie v radiotekhnike (Theory of Nonuniform Lines and Their Application in Electronics) Moscow, Sov. radio, 1964.
[46] W. A. S. Lamb, IRE Trans. Nucl. Sci. NS-9, 57 (1962).
[47] I. G. Kataev, Udarnye élektromagnitnye volny (Electromagnetic Shock Waves), Moscow, Sov. radio, 1963.
[48] I. N. Meshkov and B. V. Chirikov, Zh. Éksp. Tekh. Fiz. **35**, 2202 (1965) [Sov. Phys. Tech. Phys. **10**, 1688 (1966)].
[49] P. S. Antsupov et al., Preprint, JINR R9-4498, Dubna, 1969.
[50] W. A. Sherwood, IEEE Trans. Nucl. Sci. NS-14, 928 (1967).
[51] J. W. Beal, Proc. of the 1968 Proton Linear Accelerator Conference (Upton, May 20—24, 1968), N. Y., BNL, 1968, p. 713.
[52] V. K. Neil and R. K. Cooper, Part. Accel. **1**, 111 (1970).
[53] C. H. Woods, Rev. Sci. Instr. **41**, 959 (1970).
[54] Yu. P. Vakhrushin and V. S. Kuznetsov, Zh. Tekh. Fiz. **39**, 506 (1969) [Sov. Phys.-Tech. Phys. **14**, 374 (1969)].
[55] I. M. Matora et al., Preprint, JINR R9-6528, Dubna, 1970.
[56] Yu. Vakhrushin et al., Preprint, JINR R9-5714, Dubna, 1971.
[57] Yu. P. Vakhrushin et al., Trudy VII Mezhdunarodnoĭ konferentsii po uskoritelyam zaryazhennykh chastits vysokikh energiĭ (Proceedings VII Intern. Conf. on High-Energy Charged Particle Accelerators), Erevan, 1969, v. 1, Erevan, Academy of Sciences, Armenian SSR, 1970; Yu. P. Vakhrushin et al., Atomnaya énergiya **31**, 294 (1971) [Sov. Atomic Energy].
[58] R. W. Allison et al., IEEE Trans. Nucl. Sci. NS-16, No. 3, 1055 (1969).
[59] V. S. Kuznetsov et al., Preprint, Research Institute of Electrophysical Apparatus, D-0111, Leningrad, 1970.
[60] E. I. Lutsenko et al., Zh. Eksp. Teor. Fiz. **57**, 1575 (1969) [Sov. Phys.-JETP **30**, 853 (1970)]; E. I. Lutsenko et al., Zh. Tekh. Fiz. **40**, 529 (1970) [Sov. Phys.-Tech. Phys. **15**, 410 (1970)].
[61] R. Avery et al., IEEE Trans. Nucl. Sci. NS-18, No. 3, 479 (1971).
[62] G. I. Zhileĭko, Vysokovol'tnye élektronnye luchki (High Voltage Electron Beams), Moscow, Energiya, 1968.
[63] P. V. Bukaev et al., Preprint, Research Institute of Electrophysical Apparatus, A-0118, Leningrad, 1971.
[64] Yu. P. Vakhrushin et al., Preprint, JINR, 9-3288-2, Dubna, 1967.
[65] G. A. Mesyats et al., Formirovanie nanosekundnykh impul'sov vysokogo napryazheniya (Shaping of High-Voltage Nanosecond Pulses), Moscow, Énergiya, 1970.
[66] O. S. Bogdanov et al., Preprint, Research Institute of Electrophysical Apparatus, A-0112, Leningrad, 1970.
[67] V. M. Levin et al., Annotatsii dokladov, predstavlennykh na 2-e Vsesoyuznoe soveshchanie po uskoritelyam zaryazhennykh chastits (Abstracts of Reports Presented at the Second All-Union Conf. on Charged Particle Accelerators), November 11—18, 1970, Moscow, Academy of Sciences, USSR, and State Committee on Use of Atomic Energy, 1970, p. 40.

Translated by C. S. Robinson